Organic & Biomolecular Chemistry

ROYAL SOCIETY OF CHEMISTRY

PAPER

View Article Online
View Journal | View Issue

Cite this: *Org. Biomol. Chem.*, 2021, **19**, 6834

Generation of a quenched phosphonate activity-based probe for labelling the active KLK7 protease†

Evangelos Bisyris, [a] Eleni Zingkou,[a] Golfo G. Kordopati, [a] Minos Matsoukas, [a] Plato A. Magriotis, [a] Georgios Pampalakis *[b] and Georgia Sotiropoulou *[a]

Received 1st July 2021,
Accepted 19th July 2021

DOI: 10.1039/d1ob01273h

rsc.li/obc

Kallikrein 7 (KLK7) is a chymotrypsin-like serine protease with established roles in skin diseases like the rare Netherton syndrome, an overdesquamating and inflammatory condition, but also common atopic dermatitis, and a potential drug target for these and possibly other diseases. Nevertheless, tools to determine the active KLK7 enzyme are not available. Here, a mixed alkyl aryl phosphonate quenched activity-based probe that detects the active KLK7 was developed and evaluated *in vitro*. This KLK7-qABP can potentially be used to monitor KLK7 activity *in vivo*.

Introduction

Originally, the human KLK7 was discovered in the stratum corneum, the outermost layer of the epidermis, as a chymotrypsin-like serine protease and was named stratum corneum chymotryptic enzyme (SCCE).[1] KLK7 is expressed in the epidermis, where it is produced and secreted by keratinocytes at the stratum granulosum, as an inactive proenzyme (proKLK7) that requires activation. The KLK5 trypsin-like protease was identified as the main activator of proKLK7, in the context of a proteolytic cascade in the epidermis, that engages mainly KLKs but also other proteases.[2,3] KLK7 cleaves protein components of corneodesmosomes, which are intercellular junctions that maintain corneocytes bound in the stratum corneum. Specifically, KLK7 cleaves the corneodesmosin and desmocollin 1 proteins, thus, it enhances corneocyte shedding (desquamation).[2] Aberrantly elevated KLK7 activity has been linked to pathological skin overdesquamation and inflammation. In the epidermis, KLK7 also regulates lipid metabolism by degrading the enzymes acidic sphingomyelinase and β-glucocerebrosidase.[4]

The importance of KLK7 in skin (patho)physiology is supported by a number of *in vivo* studies. For example, Tg-*KLK7* mice exhibit increased epidermal inflammation and atopic dermatitis-like symptoms.[5] In accordance, KLK7 expression is increased in the epidermis of atopic dermatitis and Netherton syndrome patients.[6] Netherton syndrome is a severe type of ichthyosis caused by inherited inactivating mutations in the *SPINK5* gene encoding the multidomain serine protease inhibitor LEKTI. It is established that LEKTI deficiency results in unopposed proteolytic activities in the epidermis, mainly as a consequence of KLK5 and KLK7 hyperactivation. This aberrantly elevated proteolysis leads to epidermal overdesquamation and constitutive inflammation resulting in a severely compromised (potentially lethal) skin barrier defect. *Spink5*$^{-/-}$ mice reproduce the major cutaneous symptoms of Netherton syndrome; these mice die uniformly within a few hours after birth. Deletion of *Klk5* in *Spink5*$^{-/-}$ rescues neonatal lethality,[7–9] nevertheless, *Spink5*$^{-/-}$*Klk5*$^{-/-}$ mice do not survive beyond a few months and the majority of them die in a week, due to elevated epidermal desquamation and inflammation resulting from Klk7 activity.[8,9]

On the other hand, KLK7 displays aberrant expression in cancer, in particular, pancreatic adenocarcinomas[10] and may promote pancreatic cancer by cleaving the intercellular adhesion protein desmoglein 2[11] or by inducing E-cadherin shedding.[10] KLK7 is also overexpressed in ovarian cancer,[12] and it is considered to promote ovarian cancer by activating matrix metalloproteinases and *via* induction of IGF signaling following degradation of IGFBPs by KLK7.[13] Recently, KLK7 was shown to attenuate the symptoms of Alzheimer's disease *in vivo*.[14] Thus, the detection and monitoring of KLK7 activity is quite important for a variety of diagnostic and research applications.

Activity-based probes (ABPs) are small organic molecules that covalently bind and label only the active form of their

[a]*Department of Pharmacy, School of Health Sciences, University of Patras, Rion-Patras, 265 04, Greece. E-mail: gdsotiro@upatras.gr*
[b]*Department of Pharmacognosy-Pharmacology, School of Pharmacy, Aristotle University of Thessaloniki, Thessaloniki, 541 24, Greece. E-mail: gpampalakis@pharm.auth.gr*

†Electronic supplementary information (ESI) available. See DOI: 10.1039/d1ob01273h

target enzyme(s). To label serine proteases, various classes of ABPs have been developed of which the most important are the phosphonates that resemble the transition state analogues of known serine protease substrates during their hydrolysis reaction.[15] Initially, phosphonate ABPs were designed to bind serine proteases overall, with no specificity for distinct enzymes of this family.[16,17] Nonetheless, the specificity of phosphonates towards a certain protease can be increased by introducing a protease-specific recognition sequence between the phosphorus atom (warhead) and the detection tag.

Results and discussion

Using an *in silico* approach to screen the MEROPS database (http://www.ebi.ac.uk/merops), we identified the dipeptide sequence Phe–Phe as a specific recognition sequence for cleavage by KLK7.[18] This sequence was modified here to yield a quenched ABP (qABP) that emits fluorescence upon binding to the active (mature) KLK7 (Fig. 1 and 2).

For this, a Cy5 fluorescent moiety was added to the N-terminus, while the Phe at the C-terminus was modified to phosphono-phenylalanine and a mixed aryl-, alkyl-phosphonate ester was generated bearing the QSY21 quencher at the aryl leaving group (Fig. 2A). The synthesis and chemical formula of the compound, as well the labeling mechanism, are shown in Fig. 1 and 2. Briefly, the qABP **15** was synthesized by the Oleksyszyn reaction between benzyl carbamate (**1**), 2-phenylacetaldehyde (**2**), and triphenyl phosphite (**3**) in dichloromethane (DCM), as the first step, using copper triflate as catalyst,[19] to yield the diphenyl phosphonate Z-Phe^{P}-$(OPh)_2$ (**4**). Compound **4** was transesterified to Z-Phe^{P}-$(OEt)_2$ (**5**) with ethanol using potassium fluoride and 18-crown-6 ether as catalysts. Compound **5** reacted with oxalyl chloride to form the monochlorinated intermediate product **6**.[20] Tyramine [Tya, 4-(2-aminoethyl) phenol] (**7**) was selected as a spacer between the phosphorus atom and the quencher. Both the fluorophore

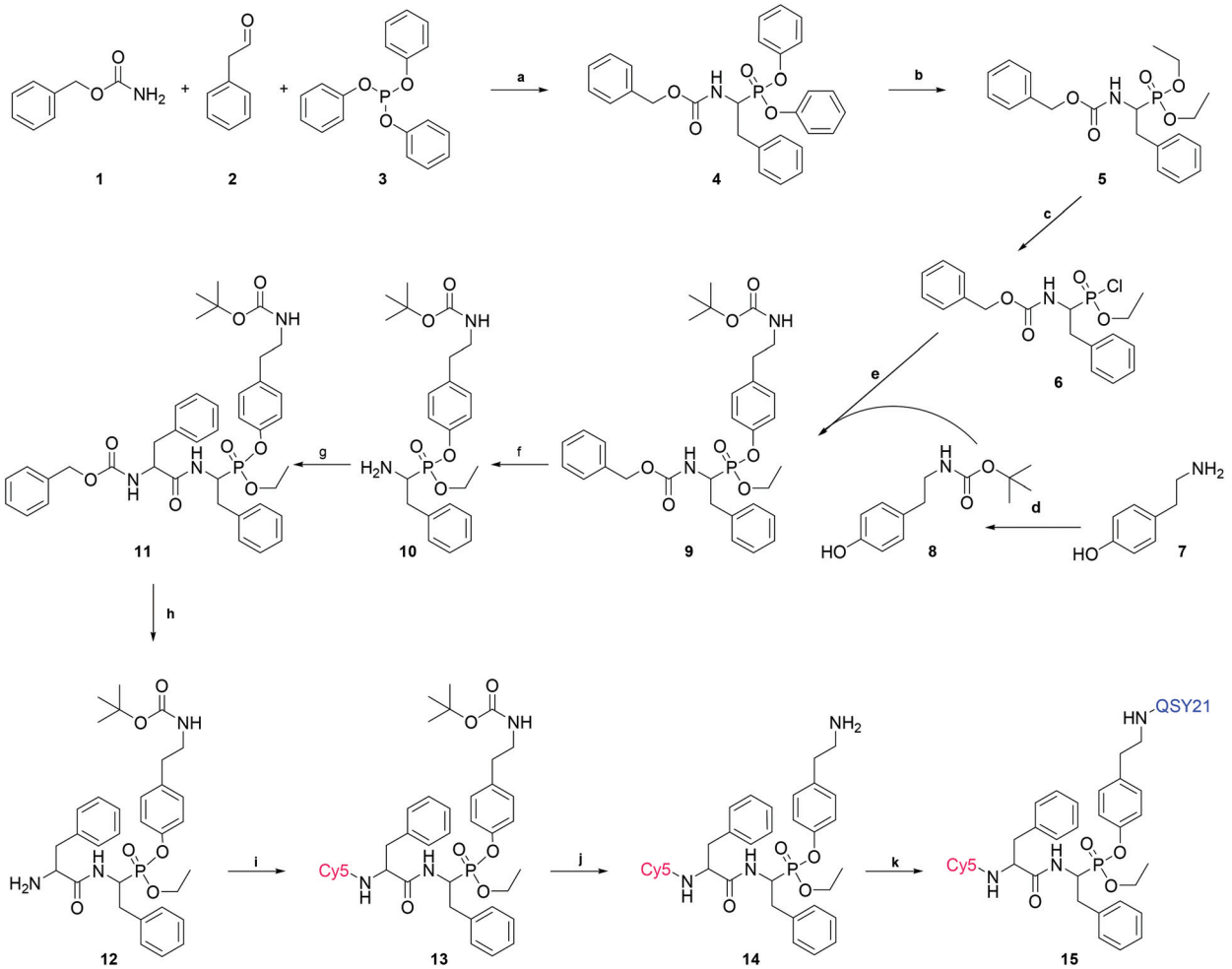

Fig. 1 Chemical synthesis of the qABP **15**. Reagents and conditions: (a) $Cu(OTf)_2$ in DCM, 56%; (b) $KF{\cdot}2H_2O$, 18-crown-6 ether in EtOH, 49%; (c) $(COCl)_2$, cat. DMF in DCM; (d) Na_2CO_3, di-*tert*-butyl dicarbonate in dioxane/water (1 : 1), 97%; (e) **8**, Et_3N in toluene, 11% for two steps (c and e); (f) TES, 10% Pd/C in MeOH; (g) Z-Phe-OH, TBTU, HOBt, DIPEA in DCM, 47% for two steps (f and g); (h) TES, 10% Pd/C in MeOH; (i) Cy5-NHS, DIPEA in DMSO, 25% for two steps (h and i); (j) TFA/DCM 1 : 1; (k) QSY21-NHS, DIPEA in DMSO, 65% for two steps (j and k).

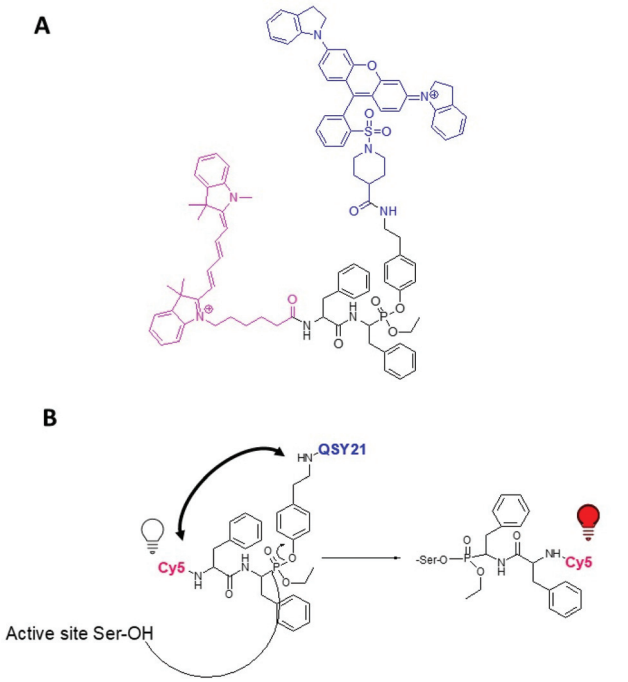

Fig. 2 (A) Chemical structure of the designed and synthesized qABP **15**. (B) Mechanism of qABP **15** reaction with a serine protease.

(Cy5) and the quencher (QSY21) were attached to amino-groups, thus, chemical synthesis proceeded by use of an orthogonal Z/Boc protection strategy. Specifically, the amino-group of compound **7** was protected with the *tert*-butyloxycarbonyl group (Boc) to yield Boc-Tya-OH (**8**). Then, **8** reacted with **6** in toluene with triethylamine to yield Z-Phe^{P}-(OEt)(OTya-Boc) (**9**). Compound **9** was deprotected with triethylsilane and 10% Pd/C in methanol to **10** that was coupled with Z-Phe-OH in DCM using 2-(1*H*-benzotriazole-1-yl)-1,1,3,3-tetraethylaminium tetrafluoroborate (TBTU)/1-hydroxybenzotriazole hydrate (HOBt) as coupling reagents, in the presence of diisopropylethylamine, to yield the *Z*-protected phosphonate Z-Phe-Phe^{P}-(OEt)(OTya-Boc) (**11**) that was purified by silica gel column chromatography. **11** was deprotected with triethylsilane and 10% Pd/C in methanol to **12**. Then, **12** reacted with Cyanine®5-NHS (Cy5-NHS) in DMSO to yield Cy5-Phe-Phe^{P}-(OEt)(Tya-Boc) (**13**) that was purified by RP-HPLC using C-18 column. Compound **13** was deprotected in 50% trifluoracetic acid/DCM to **14**, which reacted with QSY®21 succinimidyl ester (QSY21-NHS) in DMSO to yield the final qABP (**15**), that was purified with RP-HPLC using a C-18 column and lyophilized.

The successfully synthesized qABP **15** was tested for its quenching efficiency and for labelling *in vitro* the prototype enzyme chymotrypsin A. Fig. 3 shows that qABP does not exhibit increased fluorescence with increasing concentration in contrast to the non-quenched ABP **13**. As shown in Fig. 4, the qABP **15** could bind to chymotrypsin A and the fluorescence emitted by the chymotrypsin-qABP adduct was detected by scanning the SDS-PAGE gel with a

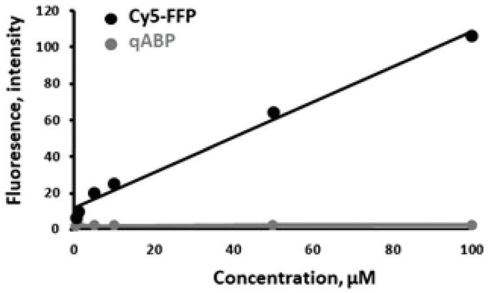

Fig. 3 Quenching efficiency. Fluorescence of increasing concentrations of qABP **15** and non-quenched Cy5-FFP (ABP **13**) was measured. No increase in the fluorescent signal for the qABP **15** relative to concentration was noted.

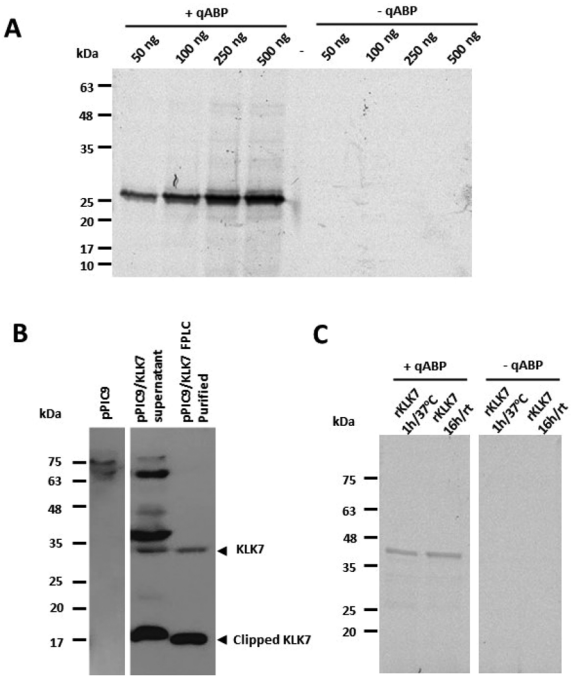

Fig. 4 (A) Detection of chymotrypsin-ABP adduct by SDS-PAGE. Chymotrypsin A (α-CT) reacted with qABP **15** at 1 mM for 1 hour at 37 °C. The gel was scanned with a Phosphorimager. (B) Active human recombinant KLK7 produced in *Pichia pastoris*. The detection was carried out by western blotting with anti-KLK7 antibody (Abcam, ab96710). (C) Detection of active recombinant KLK7 with qABP 15. Reactions in the absence of the qABP served as negative controls. rt, room temperature.

Phosphorimager. No background fluorescence was detected. Then, the qABP **15** was tested against human KLK7. Active recombinant KLK7 was expressed in the methylotrophic yeast *Pichia pastoris*. Briefly, the cDNA encoding the mature (active) KLK7 was amplified from normal human keratinocytes by RT-PCR and cloned into the pPIC9 yeast expression vector, in frame with the yeast secretion signal known as the α-factor. The pPIC9/KLK7 expression construct was linearized by digestion with *Sal*I and used for transformation of *P. pastoris* spher-

oplasts.[21] Stably transformed clones were selected based on their ability to grow in the absence of histidine and the production of KLK7 was induced by addition of methanol. KLK7 was purified from the yeast supernatant by strong cation exchange chromatography (Bio-Scale Mini Macro-prep High S, Bio-Rad) by an FPLC system (NGC Quest 10, Bio-Rad). We observed that KLK7 is widely clipped probably through self-cleavage as described.[22]

In Fig. 4, it is shown that the qABP **15** selectively detects the active form of KLK7 and not the cleaved/clipped inactive form detected by a KLK7-specific antibody. The strong upper band of ~38 kDa likely corresponds to glycosylated form of KLK7 and it is not observed following purification assumingly due to highly efficient autocatalytic cleavage which accounts for the very low yield during KLK7 purification.

Further, recombinant proKLK7 expressed in mammalian cells (R&D 2624-SE) and activated with thermolysin was reacted with the qABP at increasing amounts to determine the detection limit, which was 10 ng of active KLK7 (Fig. 5A). Consistently, enhanced intensity of the band corresponding to the active KLK7 was detected with increasing reaction times of KLK7 with the qABP, **15** as shown in Fig. 5B.

To investigate whether addition of the bulky organic groups (Cy5 and QSY21) could alter the kinetics of qABP binding onto active KLK7 as compared to the Boc-FFP[18] and the Cy5-FFP ABP (compound **13**), the IC_{50} values were determined. As shown in Table 1, the IC_{50} for qABP **15** was approximately

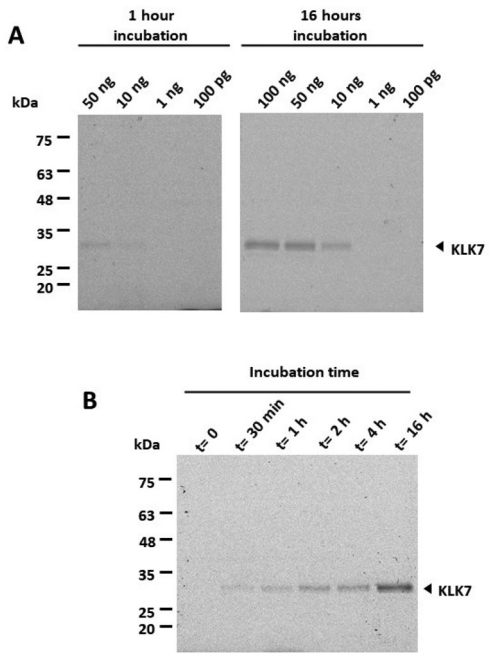

Fig. 5 Limit of detection and quenching of fluorescence at different time points. (A) Varying amounts of active recombinant KLK7 were incubated with 1 mM qABP **15** for 1 hour or 16 hours at rt. (B) 100 ng of active KLK7 were reacted with 1 mM qABP **15** for increasing time periods. It is shown that the active KLK7 can be detected after 30 min.

Table 1 IC_{50} values for the KLK7 ABPs

Compound	IC_{50}, μM
Boc-FFP	2.9 ± 1.1
Cy5-FFP (**13**)	24.2 ± 2.7
qABP (**15**)	1928.8 ± 205

80-fold higher than the IC_{50} for the Cy5-FFP that lacks the quencher.

Therefore, the addition of the bulky QSY21 group significantly reduces binding to the active KLK7. To assess the binding mode of compound **13** and the roles of Cy5 and QSY21 in compound **15**, docking calculations were performed towards the binding sites of chymotrypsin A and KLK7. Compounds **13** and **15** are racemic mixtures with R and S diastereomers at the α-carbon atom and at the phosphorus atom. Regarding the carbon stereocenter, we have previously showed that the R state is prevalent.[18] In respect to the P atom stereochemistry, the R diastereomer of compound **13** showed much higher binding scores towards both chymotrypsin A (Fig. 6A) and KLK7 (Fig. 6B). Overall, these dockings are consistent in terms of general docking orientation in respect to similar compounds described in our previous work.[18] The Cy5 group interacts with the same region of KLK7 as well as chymotrypsin A, namely S1′. Notable differences are the benzyl – F218 and *tert*-butyl – W215 and L175 interactions with KLK7 (Fig. 6B).

Regarding the qABP (compound **15**), experimental data also show a preference to chymotrypsin A. Similarly with **13**, the R isomer at the P atom in compound **15** is the prevalent. Docking calculations of compound **13**, already suggest that addition of the QSY21 group at the *tert*-butyl side of the **13** may be performed without interfering with the general binding orientation in chymotrypsin A (Fig. 6A), in contrast with KLK7, in which the *tert*-butyl group is buried in a hydrophobic area formed by W215 and L175 (Fig. 6B), potentially limiting its labelling efficiency. Furthermore, our docking suggests that in chymotrypsin A, probe QSY21 may interact in the extended surface of the protein, with two hydrophobic subpockets, formed by Y171 and W172, as well as V17 and R145 (Fig. 6C).

Collectively, these data explain why a high concentration, namely 1 mM qABP, is needed to label the active KLK7 protease. Similarly, the only reported phosphonate qABP[23] was demonstrated to react with high concentrations of trypsin *i.e.* 50 μg ml^{-1}. Further, it is known that incorporation of the large DABCYL quencher group directly to the leaving group reduces the potency of a qABP specific for cathepsins L and B. The same holds for the QSY7 quencher.[24]

Then, the cross-reactivity of qABP **15** with other related to KLK7 serine proteases was tested (Fig. 7). qABP **15** reacted with KLK7 and chymotrypsin A, while a weaker signal was detected with active KLK14. This finding indicates that the qABP **15** is specific for the KLK7 protease.

To this end, the qABP **15** was used to detect the endogenous active KLK7 from biological samples. As mentioned, KLK7

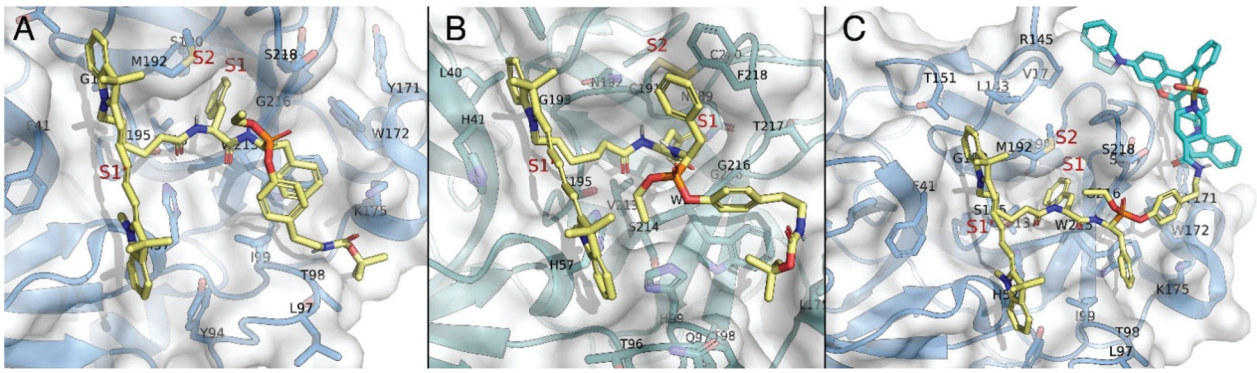

Fig. 6 (A) Docking pose of ABP **13** (yellow) bound to the catalytic site of chymotrypsin A (blue). (B) Docking pose of ABP **13** (yellow) bound to the catalytic site of KLK7 (teal). (C) Docking pose of qABP **15** bound to the catalytic site of chymotrypsin A (blue). qABP **15** is depicted in yellow except from the QSY21 group, which is colored cyan.

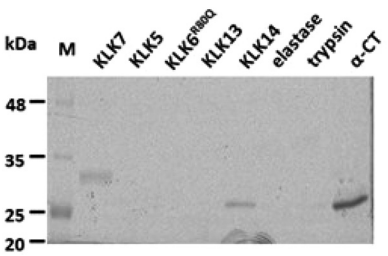

Fig. 7 Cross-reactivity of qABP 15 with other kallikreins. 1 mM qABP was allowed to react with the 100 ng enzymes for 1 hour at rt. qABP **15** showed a cross-reactivity only with KLK14.

is expressed in the stratum granulosum and is only found active at the outermost layers of the epidermis. Mouse Klk7 is localized across the epidermis of *Spink5*$^{-/-}$*Klk5*$^{-/-}$ mice, and its activity is linked to the extent of pathological overdesquamation/inflammation.[8] Indeed, as shown in Fig. 8, *Spink5*$^{-/-}$*Klk5*$^{-/-}$ mice, which overexpress KLK7 in skin compared to wt mice, exhibit enhanced qABP-emitted fluorescence

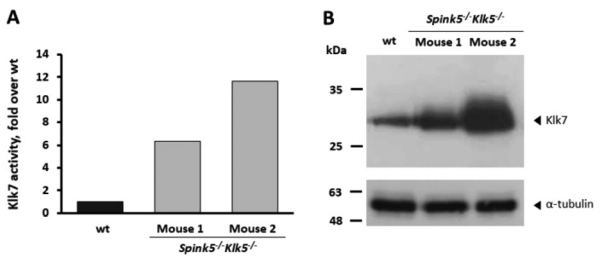

Fig. 8 Quantification of Klk7 activity by labelling with qABP 15. (A) In total, 80 μg of skin extracts were incubated with 100 μM qABP 15 for 16 hours and fluorescence was measured at λ_{em} 670 nm following excitation at λ_{exc} 633 nm in a PerkinElmer fluorimeter. (B) Detection of Klk7 (upper) and α-tubulin (lower) in mice skin extracts by western blotting using a goat anti-KLK7 specific antibody (R&D AF2624). 1, 2 indicate two different *Spink5*$^{-/-}$*Klk5*$^{-/-}$ mice. Total protein of 25 μg was loaded. No clipped Klk7 was detected, since the R&D antibody does not recognize the clipped form of KLK7/Klk7 like Abcam antibody shown in Fig. 2.

compared to wt. Elevated amounts of the KLK7 protein in the skin of *Spink5*$^{-/-}$*Klk5*$^{-/-}$ correlate with enhanced Klk7 proteolytic activity, shown for the first time here.

Conclusions

Until now, qABPs have been developed for cysteine proteases,[25] while only one study has produced two qABPs that target serine proteases, namely the neutrophil elastase and trypsin.[22] Here, we expand the use of qABPs to other physiologically relevant serine proteases by successfully demonstrating the labelling of the active KLK7. The qABP **15** was designed based on a mixed aryl alkyl phosphonate reactive warhead carrying a Phe-Phe recognition sequence.[18] It is shown that the KLK7-qABP binds both the recombinant and endogenously expressed human KLK7 but also the mouse KLK7, which makes it a useful tool for preclinical studies employing animal models, as well. The advantage of the generated qABP for future applications in molecular imaging is the use of a quencher that zeroes background fluorescence for the unbound qABP, thus, optimizing the quantification of the active enzyme based on fluorescence emission by the active enzyme-bound qABP. This is the first tool for determination and localization of active KLK7, which opens a wide array of potential analytical, (pre) clinical and diagnostic applications.

Experimental

Chemicals and spectra acquisition

Cy5-NHS and QSY®21 were obtained from Abcam and Invitrogen, respectively. All the others chemical reagents and solvents were purchased from Sigma-Aldrich and were used without further purification. Silica gel chromatography was performed using glass columns packed with silica gel 60 (220–400 mesh). Analytical thin-layer chromatography (TLC) was performed on 0.25 mm Merck silica gel 60 F_{254} plates and visualized by UV light at 254 nm and/or stained with ninhydrin

spray (Kaiser test). Nuclear magnetic resonance (NMR) spectra were recorded on a Bruker AVANCE II spectrometer at 600 MHz for ^{1}H, 151 MHz for ^{13}C, and 243 MHz for ^{31}P in $CDCl_3$ or CD_3OD. The proton chemical shift values are reported in parts per million (ppm) downfield from tetramethylsilane and referenced to the residual proton resonance of $CDCl_3$ (δ 7.26) or CD_3OD (δ 3.31). The carbon chemical shift values are reported in parts per million (ppm) downfield from tetramethylsilane and referenced to the carbon resonance of $CDCl_3$ (δ 77.0). Electrospray ionization mass spectra (ESI-MS) were recorded on an Amazon SL instrument of Bruker Daltonics or a TSQ 7000 spectrometer (Electrospray Platform LC of Micromass) coupled to a MassLynx NT 2.3 data system. Analytical and semi-preparative reverse phase high performance liquid chromatography (RP-HPLC) was performed using a Waters SunFire™ C_{18} column (4.6 × 100 mm, 3.5 μm packing material) on a SHIMADZU LC-20 AD instrument.

The chemical synthesis, NMR and MS spectra are described and shown in detail in ESI.†

Biological assessment

Ethics. All experiments were performed in compliance with the author's institute' policy on animal use and ethics. Animal experiments were carried out in the approved EL13-BIOexp-04 facilities of the University of Patras and the protocol was approved by the local committee (Veterinary Department of Regional Units of Achaia, Region of Western Greece; Protocol 187537/627).

Mouse samples. The generation of *Spink5*$^{-/-}$*Klk5*$^{-/-}$ mice has been described previously.[7] Approximately 10 mg of skin tissue was pulverized under liquid N_2 with a pestle and mortar and RIPA lysis buffer was added (25 mM Tris-HCl, pH 7.6, 150 mM NaCl, 1% NP-40, 0.5% sodium deoxycholate and 0.1% SDS), then, incubated on ice for 30 min, centrifuged at 4000 rcf at 4 °C for 10 min and finally supernatants were collected, and protein concentration was determined by Bradford assay.

Proteins. The recombinant KLK6^{R80Q}, KLK5, and KLK13 were expressed in *Pichia pastoris* strain KM71 previously by our group.[21] ProKLK14 and proKLK7 were purchased from R&D and activated with thermolysin according to manufacturer's instructions. Trypsin and chymotrypsin A were obtained from Sigma. Elastase from pig pancreas was obtained from Thermo Fisher Scientific.

Expression and purification of recombinant KLK7. The cDNA encoding the mature (active) KLK7 was amplified by RT-PCR from total RNA extracted from normal keratinocytes using the following primers: 5′-GGCACTCGAGAAAAGAATTATTGATGGCGCCCA-3′ (forward) and 5′-GGCAGAATTCGCGTTAGCGATGCTTTTTCA-3′ (reverse). Subsequently, the PCR-amplified fragment was cloned into the pPIC9 vector between the *Xho*I and *Eco*RI sites (*underlined*). 10 μg of the pPIC9/KLK7 construct were linearized with *Sal*I and used to transform the *Pichia pastoris* strain KM71 spheroplasts, prepared as described.[21] Recombinant yeast colonies were selected based on their growth in the absence of histidine. The colonies were grown in larger liquid cultures (500 ml) and the production of KLK7 was induced with 1% CH_3OH. Then, the supernatants containing the secreted KLK7 were collected by centrifugation, dialyzed against 10 mM sodium acetate buffer pH 5.3, and purified by strong cation exchange chromatography (Bio-Scale Mini Macro-prep High S, BioRad) in an FPLC system (NGC Quest 10, BioRad).

Western blots. Recombinant KLK7 or mouse skin extracts (25 μg total protein), expressing Klk7, were resolved in a 12% SDS-PAGE and transferred onto a PVDF membrane. The membrane was blocked with 5% non-fat dry milk in PBS for 1 hour at room temperature, then, incubated for 16 hours at 4 °C with the primary antibody abcam (ab 96710) at 1 : 2500 dilution for detection of the recombinant KLK7 or the antibody from R&D (AF2624), at 1 : 200 dilution, for detection of Klk7 in mouse skin extracts. Then, secondary antibodies were added, *i.e.*, an anti-rabbit (Amersharm Biosciences, NA934) 1 : 2000 for KLK7 or an anti-goat (Millipore, AP132P) 1 : 1000 for mouse Klk7 for 1 hour at room temperature. For α-tubulin detection, the primary antibody was obtained from Sigma (T5168) and was a mouse monoclonal antibody. Finally, the immunospecific bands were visualized with enhanced chemiluminescence (Thermo scientific). The R&D antibody could detect both the human KLK7 and the mouse Klk7 orthologue proteins in contrast to abcam's antibody that only detected the human KLK7.

Labelling of proteases with the qABP. A stock solution of 100 mM qABP in DMSO was prepared. Then, chymotrypsin A or other enzymes were allowed to react with 1 mM qABP in a 20 μl reaction in PBS for 1 h at 37 °C unless otherwise indicated. Each reaction was stopped by addition of Laemmli loading buffer. Samples were then boiled, resolved on a 12% SDS-PAGE and scanned for fluorescence by a Phosphorimager (FUJIFILM fluorescent image analyzer, model FLA-3000).

Detection of active Klk7 in mouse skin extracts. 80 μg of total proteins extracted from murine total skin were pretreated with 100 μM qABP-KLK7 for 16 hours at room temperature, then, fluorescence was measured by a PerkinElmer fluorimeter at excitation/emission wavelengths of 633/670 nm. Autofluorescence intensity of qABP was almost zero indicating that the addition of quencher successfully blocked the fluorescence emitted by the Cy5.

Determination of IC_{50}. KLK7 inhibition study was carried out in assay buffer (100 mM Tris-HCl, pH 8.0, 100 mM NaCl, 0.005% Triton X-100). 12 nM KLK7 were incubated with the ABPs (500 nM–200 μM for Cy5-FFP, 50 μM–10 mM for qABP **15** and 10 nM–5 mM for Boc-FFP) for 16 hours at room temperature in the assay buffer. Then, the KHLY-pNA substrate[26] purchased from Sigma-Aldrich was added at 100 μM and absorbance was measured at 405 nm after 10 min incubation. Reaction without ABP served as the control. Data were inserted into the online available program Very Simple IC50 Tool (http://www.ic50.tk/) for fitting and calculation of the IC_{50}.

Quenching efficiency. Determination of the quenching efficiency was carried out as described previously.[24] Briefly, serial dilution from the qABP and the non-quenched analog (compound **13**) were made and the fluorescence was recorded.

Docking. The docking process on KLK7, was performed on the crystal structure of the hydrolase (PDB code 2QXG)[27] and bovine chymotrypsin A (PDB code 2P8O).[28] Compounds were docked into the binding site of the protein using AutoDock Vina and AutoDockTools[29] for partial charges calculation and file format preparation. The protease was held rigid during the docking process, while ligands were allowed to be flexible. Docking calculations were performed using a grid box with dimensions of 80 × 80 × 80 Å, a search space of 10 binding modes and exhaustiveness was set to 20. The scoring algorithm implemented was using VinaSH,[30] an improved version of AutoDock Vina, which also considers sulfur and halogen bonding into the forcefield and scoring algorithm.

Author contributions

Evangelos Bisyris: conceptualization, investigation, methodology, visualization. Plato A. Magriotis: conceptualization, methodology. Minos Matsoukas: methodology, validation. Eleni Zingkou, Golfo G. Kordopati: investigation, methodology, validation, visualization, data curation. Georgia Sotiropoulou, Georgios Pampalakis: conceptualization, validation, data curation, project administration, resources, supervision, writing original draft, funding acquisition.

Conflicts of interest

There are no conflicts to declare.

Acknowledgements

We would like to thank Professor Andriew McKenzie (MRC Laboratory of Molecular Biology, Cambridge, UK) for kindly providing the *Spink5*$^{-/-}$ mice. We acknowledge partial support of this work by the projects: [1] "BIOLUMINPD; code T1EDK-03884", which is implemented under the Call "RESEARCH-CREATE-INNOVATE" funded by the Operational Program "Competitiveness, Entrepreneurship and Innovation": (NSRF 2014-2020) and co-financed by Greece and the European Union (European Regional Development Fund) and, [2] The Hellenic Foundation for Research and Innovation (HFRI) and the General Secretariat for Research and Innovation (GSRI), under grant agreement no. 1876.

Notes and references

1 A. Lundstrom and T. Egelrud, *Acta Derm.-Venereol.*, 1991, **71**, 471–474.
2 C. Caubet, N. Jonca, M. Brattsand, M. Guerrin, D. Bernard, R. Schmidt, T. Egelrud, M. Simon and G. Serre, *J. Invest. Dermatol.*, 2004, **122**, 1235–1244; C. A. Borgoño, I. P. Michael, N. Komatsu, A. Jayakumar, R. Kapadia, G. L. Clayman, G. Sotiropoulou and E. P. Diamandis, *J. Biol. Chem.*, 2007, **282**, 3640–3652.
3 G. Pampalakis and G. Sotiropoulou, *Biochim. Biophys. Acta*, 2007, **1776**, 22–31; G. Sotiropoulou, E. Zingkou and G. Pampalakis, *Exp. Dermatol.*, 2021, **30**, 628–644; G. Sotiropoulou and G. Pampalakis, *Biol. Chem.*, 2010, **391**, 321–331.
4 J. P. Hachem, M. Q. Man, D. Crumrine, Y. Uchida, B. E. Brown, V. Rogiers, D. Roseeuw, K. R. Feingold and P. M. Elias, *J. Invest. Dermatol.*, 2005, **125**, 510–520.
5 L. Hansson, A. Bäckman, A. Ny, M. Edlund, E. Ekholm, B. E. Hammarström, J. Törnell, P. Wallbrandt, H. Wennbo and T. Egelrud, *J. Invest. Dermatol.*, 2002, **118**, 444–449.
6 N. Komatsu, K. Saijoh, C. Kuk, A. C. Liu, S. Khan, F. Shirasaki, K. Takehara and E. P. Diamandis, *Exp. Dermatol.*, 2007, **16**, 513–519; N. Komatsu, M. Tanaka, N. Otsuki, R. Ohka, O. Amano, K. Takehara and K. Saijoh, *J. Invest. Dermatol.*, 2002, **118**, 436–443.
7 L. Furio, G. Pampalakis, I. P. Michael, A. Nagy, G. Sotiropoulou and A. Hovnanian, *PLoS Genet.*, 2015, **11**, e1005389.
8 P. Kasparek, Z. Ileninova, O. Zbodakova, I. Kanchev, O. Benada, K. Chalupsky, M. Brattsand, I. M. Beck and R. Sedlacek, *PLoS Genet.*, 2017, **13**, e1006566.
9 E. Zingkou, G. Pampalakis and G. Sotiropoulou, *Biochim. Biophys. Acta, Mol. Basis Dis.*, 2020, **1866**, 165831.
10 S. K. Johnson, V. C. Ramani, L. Hennings and R. S. Haun, *Cancer*, 2007, **109**, 1811–1820.
11 V. C. Ramani, L. Hennings and R. S. Haun, *BMC Cancer*, 2008, **8**, 373.
12 E. Chen, H. Zhu, Y. Yang, L. Wang, J. Zhang, Y. Han and X. Liu, *Open Med.*, 2020, **15**, 932–939.
13 L. M. Silva, T. Stoll, T. Kryza, C. R. Stephens, M. L. Hastie, H. F. Irving-Rodgers, Y. Dong, J. J. Gorman and J. A. Clements, *Sci. Rep.*, 2017, **7**, 6789.
14 K. Kidana, T. Tatebe, K. Ito, N. Hara, A. Kakita, T. Saito, S. Takatori, Y. Ouchi, T. Ikeuchi, M. Makino, T. C. Saido, M. Akishita, T. Iwatsubo, Y. Hori and T. Tomita, *EMBO Mol. Med.*, 2018, **10**, e8184.
15 M. Fonović and M. Bogyo, *Expert Rev. Proteomics*, 2008, **5**, 721–730.
16 Y. Liu, M. P. Patricelli and B. F. Cravatt, *Proc. Natl. Acad. Sci. U. S. A.*, 1999, **96**, 14694–14699.
17 G. Pampalakis, E. Zingkou, K. Vekrellis and G. Sotiropoulou, *Chem. Commun.*, 2017, **53**, 3246–3248.
18 E. Bisyris, E. Zingkou, G. G. Kordopati, M. Matsoukas, P. A. Magriotis, G. Pampalakis and G. Sotiropoulou, *Chem. Commun.*, 2021, **57**, 6507–6510.
19 J. Joossens, P. Van der Veken, A. M. Lambeir, K. Augustyns and A. Haemers, *J. Med. Chem.*, 2004, **47**, 2411–2413; J. Oleksyszyn, L. Subotkowska and P. Mastalerz, *Synthesis*, 1979, 985–987.
20 B. J. Foust, M. M. Poe, N. A. Lentini, C. C. Hsiao, A. J. Wiemer and D. F. Wiemer, *ACS Med. Chem. Lett.*, 2017, **8**, 914–918.

21 G. Sotiropoulou, V. Rogakos, T. Tsetsenis, G. Pampalakis, N. Zafiropoulos, G. Simillides, A. Yiotakis and E. P. Diamandis, *Oncol. Res.*, 2003, **13**, 381–391.
22 Y. Yu, I. Prassas, A. Dimitromanolakis and E. P. Diamandis, *J. Biol. Chem.*, 2015, **290**, 17762–17775.
23 S. Serim, P. Baer and S. H. L. Verhelst, *Org. Biomol. Chem.*, 2015, **13**, 2293–2299.
24 G. Blum, S. R. Mullins, K. Keren, M. Fonovič, C. Jedeszko, M. J. Rice, B. F. Sloane and M. Bogyo, *Nat. Chem. Biol.*, 2005, **1**, 203–209.
25 G. Blum, G. von Degenfeld, M. J. Merchant, H. M. Blau and M. Bogyo, *Nat. Chem. Biol.*, 2007, **3**, 668–677; Y. Ben-Nun, E. Merquiol, A. Brandis, B. Turk, A. Scherz and G. Blum, *Theranostics*, 2015, **5**, 847–862.
26 S. J. de Veer, L. Furio, J. E. Swedberg, C. A. Munro, M. Brattsand, J. A. Clements, A. Hovnanian and J. M. Harris, *J. Invest. Dermatol.*, 2017, **137**, 430–439.
27 M. Debela, P. Hess, V. Magdolen, N. M. Schechter, T. Steiner, R. Huber, W. Bode and P. Goettig, *Proc. Natl. Acad. Sci. U. S. A.*, 2007, **104**, 16086–16091.
28 A. Moulin, J. J. Bell, R. F. Pratt and D. Ringe, *Biochemistry*, 2007, **46**, 5982–5990.
29 O. Trott and A. J. Olson, *J. Comput. Chem.*, 2010, **31**, 455–461.
30 J. Koebel, A. Cooper, G. Schmadeke, S. Jeon, M. Narayan and S. Sirimula, *J. Chem. Inf. Model.*, 2016, **56**, 2298–2309.